

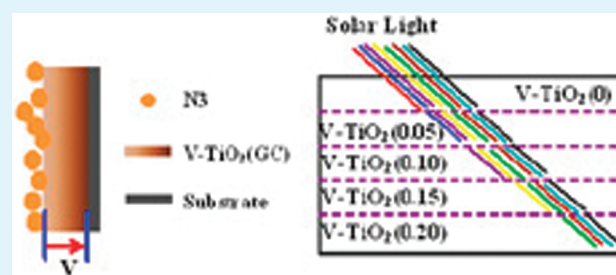
TiO₂ Photoanode Structure with Gradations in V Concentration for Dye-Sensitized Solar Cells

Zhifeng Liu,* Yabin Li, Chengcheng Liu, Jing Ya, Lei E, Wei Zhao, Dan Zhao, and Li An

Department of Materials Science and Engineering, Tianjin Institute of Urban Construction, 300384 Tianjin, China

ABSTRACT: V-TiO₂(GC) photoanode film with graduated structure was prepared in a dye-sensitized solar cell work electrode by layer-by-layer method using TiO₂ precursor with gradations in V concentration on the indium tin oxide transparent conducting glass from substrate to surface. The effects of the gradient in V concentration on the structures and properties of TiO₂ photoanode film were discussed. The structure of the gradient V concentration has remarkable influence on the final performance of the DSSCs and *I*–*V* characteristic measurement indicates an enhanced efficiency by 31% as compared to pure TiO₂ nanoparticles film samples due to abundant solar light, fast injection and transmission velocity and the slowdown recombination of photoexcited electrons, simultaneously.

KEYWORDS: V-TiO₂, photoanode, gradient, V doping, dye-sensitized solar cell



1. INTRODUCTION

Over past few years, the dye-sensitized solar cells (DSSCs) have been attracting lots of attention because of their potential for the development of low-cost and large area photovoltaics.^{1,2} Titanium dioxide (TiO₂) is a semiconductor that has been extensively utilized in photovoltaic dye-sensitized solar cells as a photoanode material. However, only 4–5% of solar light can be utilized because of the wide band gap of TiO₂ (3.0–3.2 eV). Nowadays, considerable efforts have been made in the improvement of photoelectricity by using abundant visible light. To achieve such a goal, many scientific studies have been conducted to narrow the band gap of or introduce stable optical sensitizers into TiO₂ such as doping TiO₂ with various nonmetal or metal atoms,^{3–7} semiconductor composition,^{8,9} and anchoring an organic dye sensitizer molecule on the surface of TiO₂.^{1,2} Recently, Graetzel et al. reported the nanocrystalline anatase TiO₂ photoanode modified by doping with Nb⁵⁺, which brings the power conversion efficiency to 8.7%, due to the improvement of charge collection efficiency.¹⁰ Zou et al had fabricated a La-doped TiO₂ photoanode, which gave an efficiency improved by 13.5% compared with that of the DSSCs fabricated from pure TiO₂, caused by the higher density of oxygen vacancies in TiO₂ surfaces.¹¹ Vanadium(V) has also attracted a lot of attention as a doping element due to its structure allowing the reduction of the band gap of TiO₂.^{12–15} In our previous work, the V-doped TiO₂ film was prepared on glass substrates via sol–gel method using ammonium metavanadate as V source. It was found that the band gap showed a gradual decrease from 3.28 eV to 2.82 eV with the increase of the V doping content from 0 to 0.2 in V-TiO₂.¹⁵

Moreover, many efforts were also made to study how the TiO₂ photoanode films affect the efficiency of DSSCs, such as appropriate thickness¹⁶ and porosity.¹⁷ Different particle morphologies, such as nanotubes,¹⁸ nanofibers,¹⁹ and micropores formed by

using organic template,²⁰ have also been reported. However, the recombination of the electrons injected into the TiO₂ with either the dye or the redox electrolyte hinders the DSSCs performance. A common technique to reduce the recombination rate is to create core–shell heterostructures. The energy barrier formed between the core and shell materials can reduce the recombination process.^{21–23}

In the previous research, the doping element was mostly uniformity in TiO₂ photoanode. However, in the present work, we fabricate a TiO₂ photoanode with a V gradient concentration by layer-by-layer technique and then introduce the photoanode onto the TiO₂ DSSCs to overcome the above-mentioned two limitations, i.e., absorbing abundant sun light and reducing the recombination of photoexcited electrons. To illustrate the effect of the graduated photoanode structure, a serial of nanostructures, TiO₂ and V-doped TiO₂ nanoparticles films were designed and synthesized through scalpel method. By varying the concentration of V, a systematic study on the factor that influences the photovoltaic properties of TiO₂ DSSCs is carried out. The structure of the graduated photoanode shows remarkable influence on the final performance of the DSSCs, which indicates that the conversion efficiency can be further improved by careful design of the photoanode materials.

2. EXPERIMENTAL SECTION

2.1. Preparation of Nanoparticles. In this paper, sol–gel method was used to synthesize TiO₂ nanoparticles. TiO₂ sol was prepared at room temperature as following: 30 mL of tetrabutylorthotitanate was dissolved in the mixture solution of 34.2 mL of ethanol and

Received: February 22, 2011

Accepted: April 14, 2011

Published: April 14, 2011

1 mL of acetylacetone. Stir the solution for 3 h followed by hydrolysis with addition of a mixture of 1.5 mL of deionized water, 4.3 mL of concentrated nitric acid, and 17.4 mL of ethanol dropwise. After further stirring for 2 h, the TiO_2 sol was formed. This sol was then kept in a brown glass bottle to age for 24 h at room temperature, subsequently dried at 100 °C for 24 h, and finally heated to the temperature of 550 °C for 1 h at a heating rate of 2 °C/min in air until TiO_2 nanoparticles were obtained.

$\text{V-TiO}_2(\text{x})$ nanoparticles can be fabricated by adding x mole ammonium metavanadate (NH_4VO_3) into the TiO_2 sol. It should be noted that the number x in $\text{V-TiO}_2(\text{x})$ denotes the mole of adding V in sol.

2.2. Preparation of V-TiO_2 Films. As-prepared $\text{V-TiO}_2(\text{x})$ nanoparticles were mixed with ethanol and stirred overnight, forming a colloidal suspension with the $\text{V-TiO}_2(\text{x})$ content of 20 wt %. To obtain porous structural film, we added PEG2000 into the solution. The suspension was then coated onto the indium tin oxide (ITO) glass substrate by scalpel method. This coating process was repeated several cycles until the required thickness (about 3 μm) was obtained. Using particles with different V/Ti mol ratio, a series of coatings with different values of V (i.e., 0.2, 0.15, 0.1, 0.05, and 0) in $\text{V-TiO}_2(\text{GC})$ film were formed on the surface of glass substrate. For comparison, the TiO_2 , $\text{V-TiO}_2(0.05)$, $\text{V-TiO}_2(0.1)$, $\text{V-TiO}_2(0.15)$, $\text{V-TiO}_2(0.2)$ films with similar thickness were also prepared only using the single $\text{V-TiO}_2(\text{x})$ nanoparticles. Prior to the preparation, the ITO glass substrate was ultrasonically rinsed for 15 min in acetone, iso-propyl alcohol, and ethanol absolute, respectively. After drying in air, the nanoparticles film was calcined in air up to 550 °C at a heating rate of 2 °C/min.

2.3. Assembly of Dye-Sensitized Solar Cells. The TiO_2 and $\text{V-TiO}_2(\text{GC})$ nanoparticles films, used as photoanode in DSSCs with the thickness of approximately 3 μm , were sensitized in a 0.05 mM ethanol solution of N3 dyes for at least 12 h at 60 °C. The excess unanchored dyes were rinsed off by absolute ethanol and dried in air which was then covered with a platinum sheet acted as counter electrode. The internal space of the cell was filled with liquid electrolyte (0.5 M LiI, 0.05 M I_2) dissolved in acetonitrile by capillary action. In order to further illuminate the effect of V dopant on cell performance, $\text{TiO}_2(0.2)$ and $\text{V-TiO}_2(\text{GC})$ nanoparticles films were also used as photoanode without N3 dyes. To collect accurate data, five parallel cell samples for each photoanode film were assembled and measured.

2.4. Characterization. Morphology of nanoparticles and films was observed by a PHILIPS XL-30 environment scanning electron microscopy (ESEM) and transmission electron microscopy (TEM, JEOL 100CX-II). X-ray diffraction (XRD) of nanoparticles was performed with a Rigaku D/max-2500 using $\text{Cu K}\alpha$ radiation ($\lambda = 0.154059$ nm). Optical transmittance of photoanode films was examined by DU-8B UV/vis double-beam spectrophotometer. Photocurrent of the TiO_2 DSSCs was measured under irradiation of a xenon lamp (80 mW cm^{-2}) with global AM1.5 condition, and photocurrent–voltage curves of the TiO_2 DSSCs were obtained using a potentiostat.

3. RESULTS AND DISCUSSION

Figure 1 shows SEM and TEM images of $\text{V-TiO}_2(0.2)$ nanoparticles where the size of $\text{V-TiO}_2(0.2)$ nanoparticles is about 15–20 nm. Electron diffraction pattern (Figure 1b) displays discontinuous diffraction rings. It is confirmed that this TiO_2 is polycrystalline. XRD analysis shows that the main crystal phase of all obtained nanoparticles samples has an anatase structure. The XRD patterns of TiO_2 and $\text{V-TiO}_2(0.2)$ nanoparticles are given in Figure 2. No peaks generated from vanadic oxide crystallites are visible, indicating the formation of solid solution in $\text{V-TiO}_2(\text{x})$. Based on data presented by Rodella et al, it is believed that all vanadium is incorporated into TiO_2 as vanadyl groups (V ion) rather than forms crystalline vanadic oxide.²⁴

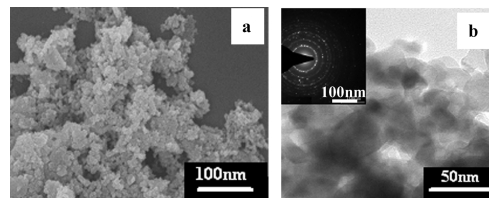


Figure 1. SEM and TEM images of $\text{V-TiO}_2(0.2)$ nanoparticles: (a) SEM; (b) TEM (the inset is SAED).

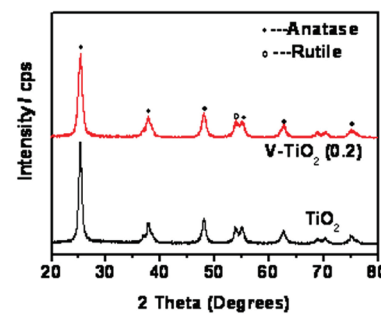


Figure 2. XRD patterns of the nanoparticles.

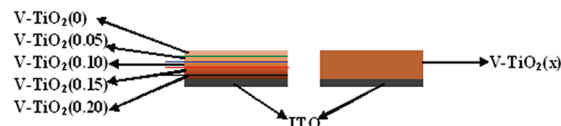


Figure 3. Schematic diagram of the $\text{V-TiO}_2(\text{GC})$ photoanode film (left) and $\text{V-TiO}_2(\text{x})$ photoanode film (right).

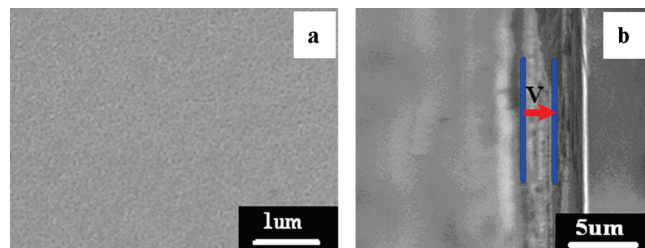


Figure 4. Top-view and cross-sectional SEM images of $\text{V-TiO}_2(\text{GC})$ nanoparticles film: (a) top-view SEM image; (b) cross-sectional SEM image.

The $\text{V-TiO}_2(\text{GC})$ photoanode with a V gradient concentration from substrate to surface was prepared by layer-by-layer technique using a colloidal suspension with different $\text{V-TiO}_2(\text{x})$ nanoparticles. Moreover, the TiO_2 , $\text{V-TiO}_2(0.05)$, $\text{V-TiO}_2(0.1)$, $\text{V-TiO}_2(0.15)$, and $\text{V-TiO}_2(0.2)$ films with similar thickness were also fabricated only using the single $\text{V-TiO}_2(\text{x})$ nanoparticles. The schematic diagram of the $\text{V-TiO}_2(\text{GC})$ photoanode film (left) and $\text{V-TiO}_2(\text{x})$ photoanode film (right) was given in Figure 3.

Figure 4 shows the top-view and cross-sectional SEM images of $\text{V-TiO}_2(\text{GC})$ nanoparticles film prepared by layer-by-layer method. The mole value of V in $\text{V-TiO}_2(\text{GC})$ is 0.2, 0.15, 0.1, 0.05, and 0 across the film from ITO glass substrate. Nanoparticles film appears very uniform and there is no cracking or deformation visible during the process of calcination. Moreover,

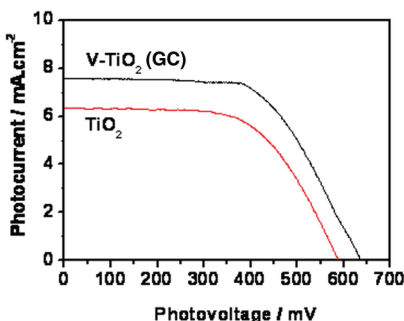


Figure 5. Photocurrent–voltage curves of the TiO_2 -based DSSCs.

Table 1. Parameters of Dye-Sensitized Solar Cell with Different Photoanode Films

photoanode film	V_{oc} (mV)	J_{sc} (mA cm^{-2})	FF (%)	η (%)
TiO_2	588	6.36	59	2.76
V-TiO_2 (GC)	637	7.57	60	3.62

in order to anchor more dye molecules, some pores were found in the film originated from the volatilization, decomposition and combustion of PEG2000.^{15,25,26}

Figure 5 presents the photocurrent–voltage curves of the DSSCs based on the TiO_2 and V-TiO_2 (GC) (V is 0.2, 0.15, 0.1, 0.015, 0 and gradient concentration in V formed from glass substrate to surface) nanoparticles films using N3 as sensitizer, while the photoelectrochemical properties of these DSSCs are listed in Tab.1. During photocurrent measurement, cell efficiency (η) can be expressed by the following equation

$$\eta = (V_{\text{oc}} J_{\text{sc}} \text{FF}) / P_{\text{in}} \quad (1)$$

$$\text{FF} = V_{\text{opt}} J_{\text{opt}} / V_{\text{oc}} J_{\text{sc}} \quad (2)$$

where P_{in} is the power of incident white light, FF is fill factor, V_{opt} and J_{opt} are voltage and current for maximum power output, and V_{oc} and J_{sc} are open-circuit photovoltage and short-circuit photocurrent, respectively.

The cell performance of the V-TiO_2 (GC) nanoparticles film DSSCs sensitized by N3 higher than TiO_2 nanoparticles film DSSCs is expected to be high. The average values of open circuit voltage (V_{oc}) and short circuit current (J_{sc}) for V-TiO_2 (GC) nanoparticles film DSSCs are 637 mV and 7.57 mA cm^{-2} , respectively. In contrast, these values are 588 mV and 6.36 mA cm^{-2} for DSSCs based on TiO_2 nanoparticles film. Moreover, the V-TiO_2 (GC) nanoparticles film DSSCs exhibits an improved efficiency by about 31% in comparison with TiO_2 nanoparticles film. All these evidence demonstrate V-TiO_2 (GC) nanoparticles film offers the better cell performance than the TiO_2 nanoparticles film.

To understand the efficiency enhancement of DSSCs with V-TiO_2 (GC) nanoparticles film, the optical transmittance of the TiO_2 , V-TiO_2 (0.05), V-TiO_2 (0.1), V-TiO_2 (0.15), and V-TiO_2 (0.2) nanoparticles films was measured. It can be seen from Figure 6 that there is no obvious difference for the optical transmittance among those V-TiO_2 (x) nanoparticles films. However, an obvious trend that the absorption edge has gradual red-shift with the increase of the V doping content. The absorption edge can be about 460 nm when the V mole concentration is 0.2 mol. The red-shift is related to following reasons: the new phase

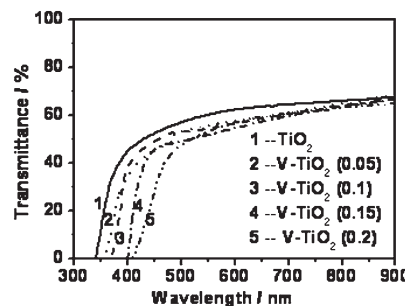


Figure 6. Optical transmittance spectra of V-TiO_2 (x) films.

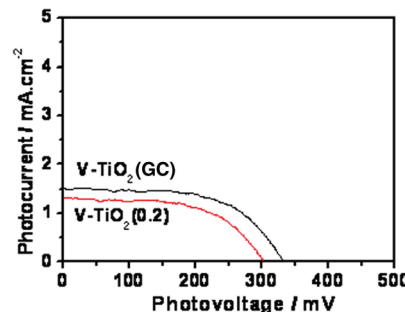


Figure 7. Photocurrent–voltage curves of the TiO_2 -based DSSCs without N3 dye.

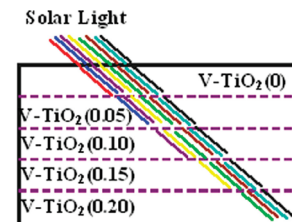


Figure 8. Schematic diagram of light utilization of the V-TiO_2 (GC) film.

of $\text{Ti}_{1-y}\text{V}_y\text{O}_2$ is formed through the replacement of V atoms to Ti atoms in TiO_2 crystal lattice due to the smaller diameter of V atom. As a result, Ti atom and O atom stay closer, which allows the photoexcited electrons easy to transit from O_{2p} to Ti_{3d} in TiO_2 .¹² The absorption coefficient α is given by the transmittance T and film thickness d using the formula $\alpha = -\ln(T)/d$. The dependence of the absorption coefficient α upon the photon energy $h\nu$ for near edge optical absorption in semiconductors takes the form $\alpha h\nu = k(h\nu - E_g)^m$, Where E_g is the optical band gap, k is a constant and $m = 1/2$ for TiO_2 with an allowed direct energy gap. On the basis of the above form, the band gap of the TiO_2 nanoparticles film is 3.3 eV, a gradual decrease with the increasing of the V content, 2.8 eV can be obtained in V-TiO_2 (0.2) nanoparticles film. It is believed that the presence of V in TiO_2 nanoparticles film is the main cause of the improved conversion efficiency of V-TiO_2 (GC) nanoparticles film DSSCs. In V-TiO_2 (GC) nanoparticles film, a graduated structure can be obtained by using different V/Ti nanoparticles, which narrow the band gap of TiO_2 and absorb more abundant solar light. As shown in Figure 8, the different solar light can be utilized by V-TiO_2 (x) layer film due to the hierarchical narrow band gap caused by doping different V in TiO_2 . It should be noted that the porous

Table 2. Cell Parameters of Different Photoanode Films without N3 Dyes

photoanode film	V_{oc} (mV)	J_{sc} (mA cm $^{-2}$)	FF (%)	η (%)
TiO ₂ (0.2)	304	1.32	57	0.28
V-TiO ₂ (GC)	334	1.52	59	0.37

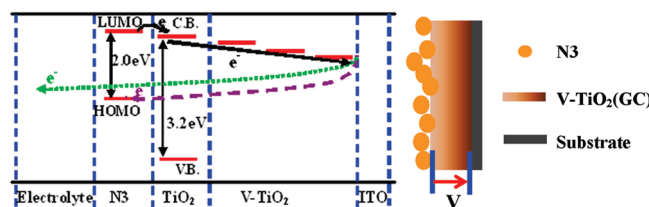


Figure 9. Schematic diagram of energy level (left) and cell structure (right) for the V-TiO₂(GC) film DSSCs.

structure caused by PEG2000 is a precondition for light transmittance in V-TiO₂(GC) nanoparticles films.

Furthermore, in order to understand the effect of V dopant on the cell performance, TiO₂(0.2) and V-TiO₂(GC) nanoparticles films were also used as photoanode without N3 dye. Figure.7 shows the photocurrent–voltage curves of the DSSCs based on the TiO₂ and V-TiO₂(GC) nanoparticles films without N3 dye as sensitizer. The photoelectrochemical properties of these DSSCs are listed in Tab.2. For the TiO₂(0.2) nanoparticles film, the η value is about 0.28, whereas for the V-TiO₂(GC) nanoparticles film, the efficiency can be improved to 0.37. The V_{oc} and J_{sc} for V-TiO₂(GC) nanoparticles film DSSCs are 334 mV and 1.32 mA cm $^{-2}$, respectively, which are much higher than those of TiO₂(0.2) nanoparticles film DSSCs (304 mV and 1.32 mA cm $^{-2}$). Thus, it can be concluded that the gradations in V concentration of TiO₂ film can improve the solar light utilization and cell performance compared with the TiO₂(0.2) nanoparticles film.

It is well-known that besides the effect of solar light utilization on the cell properties, one reason for the low conversion efficiency of traditional DSSCs is the recombination of the electrons injected into the TiO₂ with either the dye or the redox electrolyte, thereby reducing the cell efficiency. Another reason may be explained by the slow speed of injection and transmission for photoexcited electrons. The V-TiO₂(GC) photoanode structure with gradient energy band gap maybe can overcome the above two limitations. The energy band gap and cell structure of V-TiO₂(GC) can be schematically illustrated in Figure 9, where the energy band gap may be gradual decrease from film top surface to glass substrate caused by the gradient concentration of V. Just like this, the photoexcited electrons is very easy to inject from N3 to V-TiO₂(GC) and transmit in the V-TiO₂(GC) photoanodic film due to the sequential energy band of semiconductor photoanode, which significantly increases the potential current. On the other hand, the graduated structure is very efficient on retarding the back transfer of electrons and minimizing electron–hole recombination, which significantly decreases the dark current and improves the final conversion efficiency.

On the basis of the above results, it can be seen that the V-TiO₂(GC) photoanode structure with gradient V concentration shows remarkable influence on the final performance of the DSSCs. It believes that both of the following efforts are helpful for the higher conversion efficiency of V-TiO₂(GC) nanoparticles film DSSCs. First, a hierarchical narrow band structure can

be obtained by gradient V concentration in TiO₂, which can utilize more abundant solar light. Second, the photoexcited electrons is easy to inject and transmit in V-TiO₂(GC) photoanode due to the sequential heteronanostructure caused by the V gradation concentration in TiO₂. In all, the TiO₂ photoanode with gradations in V concentration is efficient on retarding the back transfer of electrons and minimizing electron–hole recombination.

Although the construction of gradient V concentration in V-TiO₂(GC) photoanode, the maximum cell efficiency is only 3.62%. Further studies are under investigation to improve the cell performances of the prepared solar cell such as changing the size and morphology of nanoparticle, thickness of film, the transmission and recombination of photoexcited electrons, and so on, which will be published in elsewhere.

4. CONCLUSIONS

V-TiO₂(GC) photoanode film with graduated structure was synthesized and assembled into a solar cell. A serial of nanostructures, TiO₂ and V-doped TiO₂ nanoparticles films, were designed and prepared by scalpel method. By varying the concentration of V, we made a systematic study on the parameters that influences the photovoltaic properties of TiO₂ DSSCs. The structure of the graduated photoanode shows remarkable influence on the final performance of the DSSCs. I – V characteristic measurement indicates an improved efficiency by 31% as compared to TiO₂ nanoparticles film samples due to advanced materials structure.

■ AUTHOR INFORMATION

Corresponding Author

*Tel: +86 22 23085236. Fax: +86 22 23085110. E-mail: tjlzf@163.com.

■ ACKNOWLEDGMENT

Authors gratefully acknowledge financial support from the Key Project of Chinese Ministry of Education (208008), China Postdoctoral Science Foundation Funded Project (20080440674), and China Postdoctoral Science Special Foundation (201003294).

■ REFERENCES

- O'Regan, B.; Gratzel, M. *Nature* **1991**, 353, 737.
- Gratzel, M. *Prog. Photovolt. Res. Appl.* **2000**, 8, 171.
- Litter, M. I. *Appl. Catal., B* **1999**, 23, 89.
- Takeuchi, M.; Yamashita, H.; Matsuoka, M.; Anpo, M.; Hirao, T.; Itoh, N.; Iwamoto, N. *Catal. Lett.* **2000**, 67, 135.
- Shahed, U. M. K.; Mofareh, A. L.; William, B. I. J. *Science* **2002**, 297, 2243.
- Chen, X. B.; Burda, C. *J. Phys. Chem. B* **2004**, 108, 15446.
- Torres, G. R.; Lindgren, T.; Lu, J.; Granqvist, C. G.; Lindquist, S. E. *J. Phys. Chem. B* **2004**, 108, 5995.
- Mor, G. K.; Varghese, O. K.; Paulose, M.; Shankar, K.; Grimes, C. A. *Sol. Energy Mater. Sol. Cells* **2006**, 90, 2011.
- Anusorn, K.; Kevin, T.; Kensuke, T.; Masaru, K.; Prashant, V. K. *J. Am. Chem. Soc.* **2008**, 130, 4007.
- Chandiran, A. K.; Sauvage, F.; Casas-Cabanas, M.; Comte, P.; Zakeeruddin, S. M.; Graetzel, M. *J. Phys. Chem. C* **2010**, 114, 15849.
- Zhang, J.; Zhao, Z.; Wang, X.; Yu, T.; Guan, J.; Yu, Z.; Li, Z.; Zou, Z. *J. Phys. Chem. C* **2010**, 114, 18396.
- Morris, D.; Dixon, R.; Jones, F. H.; Dou, Y.; Egdell, R. G.; Downes, S. W.; Beamson, G. *Phys. Rev. B* **1997**, 55, 16083.

(13) Klosek, S.; Raftery, D. *J. Phys. Chem. B* **2001**, *105*, 2815.

(14) Lee, K.; Cao, G. *J. Phys. Chem. B* **2005**, *109*, 11880.

(15) Liu, Z.; Ya, J.; E, L.; Xin, Y.; Zhao, W. *Mater. Chem. Phys.* **2010**, *120*, 277.

(16) Ito, S.; Zakeeruddin, S. M.; Baker, R. H.; Liska, P.; Charvet, R.; Comte, P.; Nazeeruddin, M. K.; Pechy, P.; Takata, M.; Miura, H.; Uchida, S.; Gratzel, M. *Adv. Mater.* **2006**, *18*, 1202.

(17) Tian, Z.; Tian, H.; Wang, X.; Yuan, S.; Zhang, J.; Zhang, X.; Yu, T.; Zou, Z. *Appl. Phys. Lett.* **2009**, *94*, 031905.

(18) Mor, G. K.; Shankar, K.; Paulose, M.; Varghese, O. K.; Grimes, C. A. *Nano Lett.* **2006**, *6*, 215.

(19) Chuangchote, S.; Sagawa, T.; Yoshikawa, S. *Appl. Phys. Lett.* **2008**, *93*, 033310.

(20) Zukalova, M.; Zukal, A.; Kavan, L.; Nazeeruddin, M. K.; Liska, P.; Gratzel, M. *Nano Lett.* **2005**, *5*, 1789.

(21) Palomares, E.; Clifford, J. N.; Haque, S. A.; Lutz, T.; Durrant, J. R. *J. Am. Chem. Soc.* **2003**, *125*, 475.

(22) Wang, Z. S.; Yanagida, M.; Sayama, K.; Sugihara, H. *Chem. Mater.* **2006**, *18*, 2912.

(23) Yu, X. L.; Song, J. G.; Fu, Y. S.; Xie, Y.; Song, X.; Sun, J.; Du, X. W. *J. Phys. Chem. C* **2010**, *114*, 2380.

(24) Rodella, C. B.; Nascente, P. A. P.; Franco, R. W. A.; Magon, C. J.; Mastelaro, V. R.; Florentino, A. O. *Phys. Status Solidi A* **2001**, *187*, 161.

(25) Liu, Z.; Jin, Z.; Li, W.; Qiu, J. *Mater. Lett.* **2005**, *59*, 3620.

(26) Liu, Z.; Li, J.; Ya, J.; Xin, Y.; Jin, Z. *Mater. Lett.* **2008**, *62*, 1190.